Study of Intense Electron Beams Produced by High-Voltage Pulsed Glow Discharges

H. F. RANEA-SANDOVAL, N. REESOR, B. T. SZAPIRO, C. MURRAY, AND J. J. ROCCA, MEMBER, IEEE

Abstract—We report the generation of high-current-density (20 A/cm^2) pulsed electron beams from high-voltage (48–100 kV) glow discharges using cathodes 7.5 cm in diameter. The pulse duration was determined by the energy of the pulse generator and varied between 0.2 μs and several microseconds, depending on the discharge current. The largest electron beam current (900 A) was obtained with an oxidized aluminum cathode in a helium–oxygen atmosphere. An oxidized magnesium cathode produced similar results, and a molybdenum cathode operated at considerably lower currents. A small-diameter (<1 mm) well-collimated beam of energetic electrons of very high current density (>1 kA/cm^2) was also observed to develop in the center of the discharge. Electrostatic probe measurements show that the negative glow plasma density and the electron beam current have a similar spatial distribution. Electron temperatures of 1–1.5 eV were measured at 7 cm from the cathode. The plasma density ($8.5 \cdot 10^{11}$ cm^{-3} at 450 A) was found to depend linearly on the discharge current. In discharges at high currents a denser and higher temperature plasma region was observed to develop at approximately 20 cm from the cathode. We have modeled the process of electron beam generation and predicted the energy distribution of the electron beam. More than 95 percent of the electron beam energy is calculated to be within 10 percent of that corresponding to the discharge voltage.

I. Introduction

GLOW DISCHARGES can be used to generate energetic beams of electrons by accelerating through the cathode fall the electrons emitted at the cathode surface by the bombardment of ions and fast neutrals [1]–[4]. There is no limit to the duration of the electron beam pulse, and it is possible to produce dc electron beams at current densities of >0.1 A/cm^2 [5]. A detailed study of pulsed high-voltage glow discharges (40–80 kV) at currents of the order of 10 mA/cm^2 was conducted by McClure [6]. O'Brien [7] has generated electron beam current densities in excess of 1 A/cm^2 over large areas, for durations of the order of 20 μs. His results were obtained using aluminum or stainless steel electrodes in different gaseous atmospheres. The largest current densities that he obtained were 5 A/cm^2 (in nitrogen at 20 mtorr) and 3 A/cm^2 (in helium at 180 mtorr). Isaacs *et al.* [8] obtained electron beam current densities up to 0.2 A/cm^2 using large-area (>1000 cm^2) aluminum cathodes in helium atmospheres up to pressures of 45 mtorr.

In the generation of dc electron beams by glow discharges it is known that oxidation of an aluminum cathode can significantly increase the electron beam current density and efficiency [3]. Surface nitridation causes a similar effect. This is a consequence of an increased secondary electron emission at the cathode surface. Thus, high secondary electron cathode materials are desirable. This work puts emphasis on studying the use of high-electron-yield cathode materials in the generation of intense pulsed electron beams.

We present in Section III results of operating aluminum and magnesium cathodes in helium, nitrogen, and oxygen atmospheres at pressures up to 720 mtorr and at voltages between 48 and 100 kV. A small amount of oxygen (<10 mtorr) was added to maintain the cathode oxidation in the helium discharges during long periods of operation. Electron beams with currents up to 900 A were produced at 65 kV using cathodes with an emitting surface area of 44 cm^2. This corresponds to a current density at the cathode of nearly 20 A/cm^2. A current density of 9 A/cm^2 was measured passing through a 7.7-μm-thick aluminum foil in the axis of the beam operating the discharge at 100 kV. The beam generation is very efficient; the electron beam current and the total discharge current were measured to differ by only a few percent. The duration of the electron beam current pulses was limited by the energy stored in the capacitors (5-nF erected capacitance) of the pulse generator. At large electron beam current densities (20 A/cm^2) the pulse duration is approximately 200 ns, while at small current densities (1 A/cm^2), it is several microseconds. We compare these results with those obtained using a molybdenum cathode that does not form a high secondary electron yield oxide or nitride layer.

In Section III-B the radial and axial distribution of the electron beam current is discussed. The radial profiles show the presence of a high-current-density (>1 kA/cm^2) small-diameter (<1 mm) beam in the axis of the discharge. This phenomenon is further discussed in Section III-D. Measurements of the plasma density and electron temperature in the negative glow region of the discharge were obtained using electrostatic probes. The

Manuscript received November 26, 1986; revised May 22, 1987. This work was supported by the U.S. Air Force. J. Rocca was supported by a National Science Foundation Presidential Young Investigators Award. B. Szapiro was supported by a fellowship from the Universidad Nacional de Buenos Aires.

The authors are with the Electrical Engineering Department, Colorado State University, Fort Collins, CO 80523. H. F. Ranea-Sandoval is on leave from Centro de Investigaciones Opticas (CIC-BA), Rep. Argentina. B. T. Szapiro is on leave from Programa de Fisica Experimental Tandil (UNCPBA), Rep. Argentina.

IEEE Log Number 8716399.

0093-3813/87/0800-0361$01.00 © 1987 IEEE

results are presented in Section III-C. The model of Section IV uses these data and predicts the electron energy distribution.

II. Experimental Apparatus

A two-stage Marx generator capable of delivering 25 J at 100 kV was built using commercially available spark-gaps, pressurized with dry nitrogen. Both stages of the Marx generator are triggered by a transmission line discharged by a third spark-gap. This spark-gap is switched by discharging a second transmission line through a grounded-grid hydrogen thyratron.

The experimental setup is schematically shown in Fig. 1. The Marx generator is enclosed in a metal tank filled with transformer oil. The vacuum chamber consists of a stainless steel cylinder 50 cm long, 20 cm ID in which the cathode is placed 13 cm from one end. The vacuum chamber is grounded and constitutes the anode of the discharge. The electron gun is connected to the Marx generator by a high-voltage high-vacuum feedthrough. The cathode holder includes a water refrigeration system for high repetition rate operation. However, most of the results presented herein were obtained at a 1-Hz repetition rate.

The vessel is pumped to 10^{-6} torr by a 200 l/s turbomolecular pump. Pressure is measured by an ionization gauge. The gases are flowed at a low rate into the chamber through needle valves, and circulated by means of a rotary pump to minimize impurities in the gas mixture. Working gas pressures are measured with a capacitance manometer.

A diagram of the electron gun is presented in Fig. 2. The cathode is enclosed in a closely spaced (1 mm) dielectric shield to avoid emission from surfaces other than the front one. The enclosure was made of polycarbonate due to its ability to support surface flashover without significant deterioration. A ceramic shield protects the plastic from direct exposure to the discharge by avoiding possible carbon sputtering from the polycarbonate, due to ion bombardment. The electron gun's structural design allows for the easy replacement of cathodes. Cathodes made of oxidized aluminum, magnesium, and molybdenum were tested. They are 7.5-cm-diameter 3.5-cm-long cylinders with rounded edges at their front surfaces.

The front cathode surfaces are hand-polished, but the results do not show any significant dependence on the surface finishing except when pores are present. Pores can cause the development of arcs on the cathode front surface, and consequently the collapse of the higher impedance glow discharge. In the case of magnesium, development of pores was observed as a consequence of the chemical attack caused by a detergent used during the cleaning procedure. After this was realized, only acetone and methanol were used as cleaning agents.

The electron beam current was measured using a commercially available pulse current monitor coil mounted inside the discharge chamber. The coil inside diameter is 5 cm. It was placed coaxial with the beam, 7 cm from the

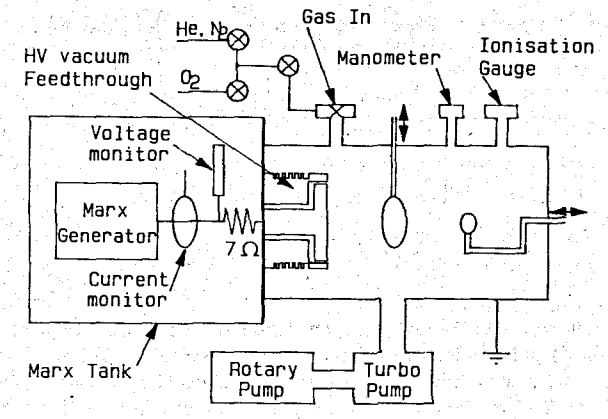

Fig. 1. Schematic diagram of the experimental apparatus. The electron beam current monitors could be alternatively replaced by movable Langmuir probes to measure electron temperature and plasma density. A 7-Ω resistor is in series with the discharge. A detailed diagram of the electron gun and high-voltage vacuum feedthrough is shown in Fig. 2.

cathode surface, and gave a signal proportional to the electron beam current passing through it. The calibrated sensitivity of the coil is 0.1 V/A. A second coil having an inner diameter of 1.25 cm and a sensitivity of 1 V/A was also used in measuring electron beam current density profiles. The coils could be displaced along the diameter of the beam by a dynamic vacuum feedthrough shown in Fig. 1. The smaller coil could also be displaced along the axis of the discharge chamber when mounted in a second vacuum feedthrough placed at the end of the chamber. The introduction of the probes in the negative glow region of the plasma, that is almost field free, does not perturb the discharge. As shown by current transmission measurements through a filtering aluminum foil, practically all (>95 percent) of the current going through the coil is composed of energetic beam electrons.

The total discharge current was measured by a third coil mounted inside the tank of the Marx generator. The discharge voltage was monitored using a 5000:1 resistive voltage divider. The plasma density and electron temperature were measured using electrostatic probes. Both single and double probes were used in these measurements. They were made of 0.25-mm-diameter tungsten wire, and were biased with batteries. Probe currents were measured with a commercially available current transformer. Spatially resolved plasma parameter measurements were obtained by displacing the probes with dynamic vacuum feedthroughs.

III. Experimental Results

A. Electron Beam Generation

Glow discharges created using three different cathode materials were studied. Cathodes made of aluminum, magnesium, and molybdenum were alternately tested in oxygen, nitrogen, and helium–oxygen atmospheres. The largest electron beam current, 900 A, was obtained at 65 kV from an aluminum cathode in a helium–oxygen gas mixture. The electronic component of the glow discharge current was measured with the 5-cm-diameter current

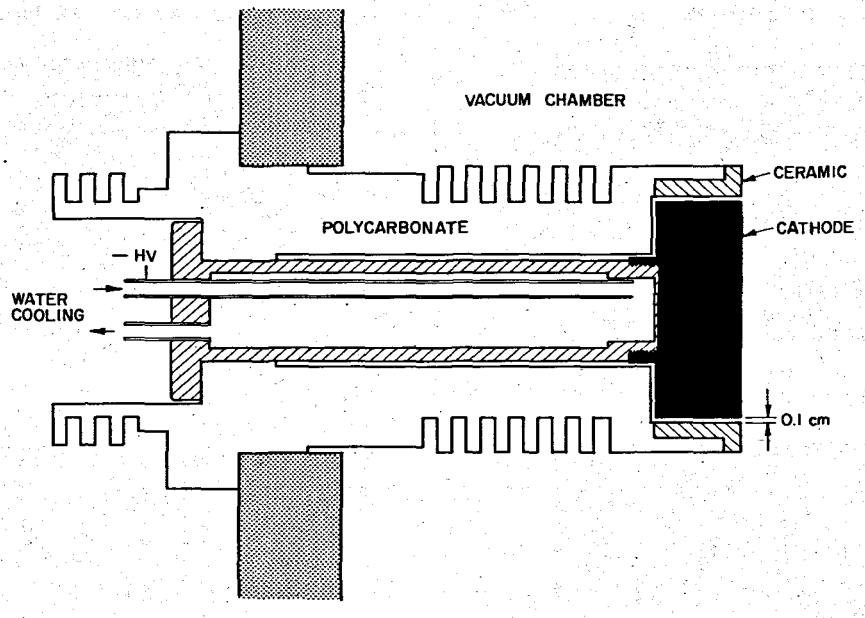

Fig. 2. Schematic diagram of the electron gun and high-voltage vacuum feedthrough. The cathode diameter is 7.5 cm.

monitoring coil placed at 7 cm from the cathode surface. The active area of the coil is 20 cm^2, approximately half of the cathode area. It is shown in Section III-B that at low currents (< 100 A) the electron beam current density distribution across the cathode is approximately uniform. Consequently, at low beam currents the electron flux measured by the coil represents nearly half of the electron beam current generated by the electron gun. At high currents, almost all the electron beam flux is measured by the coil due to the self-constriction of the electron beam, as evidenced by the fact that this current is practically equal to the total discharge current.

Fig. 3 shows the dependence of the electron beam current generated by an aluminum cathode in a helium–oxygen atmosphere on the discharge conditions. The variation of the electron beam current I (amperes) with pressure P (torr) and discharge voltage V (kilovolts) can be described by the empirical expression, $I = CV^kP^m$, where $C = (4.8 \pm 0.1)\ 10^{-3}$, $k = (3 \pm 0.15)$, and $m = (2.2 \pm 0.2)$.

The electron beam current increases sharply with increasing pressure and discharge voltage. The maximum values of voltage and pressure at which the electron beam discharge may be operated are limited by the occurrence of arcs in the gap between the cathode and the ceramic shield. At a Marx generator voltage of 65 kV, the discharge was operated at pressures up to 600 mtorr. At these conditions, the electron current measured through the monitoring coil was 900 A. This value corresponds to an electron beam current density at the cathode of approximately 20 A/cm^2. At a voltage of 100 kV the maximum operating pressure at which an electron beam was obtained was 320 mtorr, resulting in an electron beam current of 300 A.

Fig. 4(a), (b) shows a 680-A electron beam current

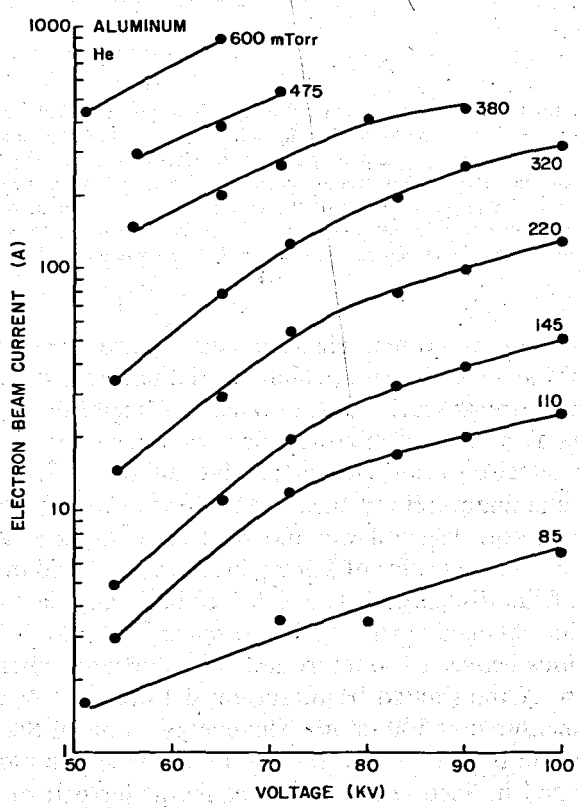

Fig. 3. Electron beam peak current versus initial voltage of the erected Marx generator, with pressure as a parameter. An aluminum cathode was used in He + 10 mtorr of O_2. A 5-cm-ID pulse transformer was used to measure the current at 7 cm from the cathode.

pulse obtained operating the discharge at a pressure of 720 mtorr and the discharge voltage for the same discharge conditions. The electron beam pulsewidth of 200 ns full width at half maximum (FWHM) is limited by the charge stored in the Marx generator. Fig. 5(a), (b) illus-

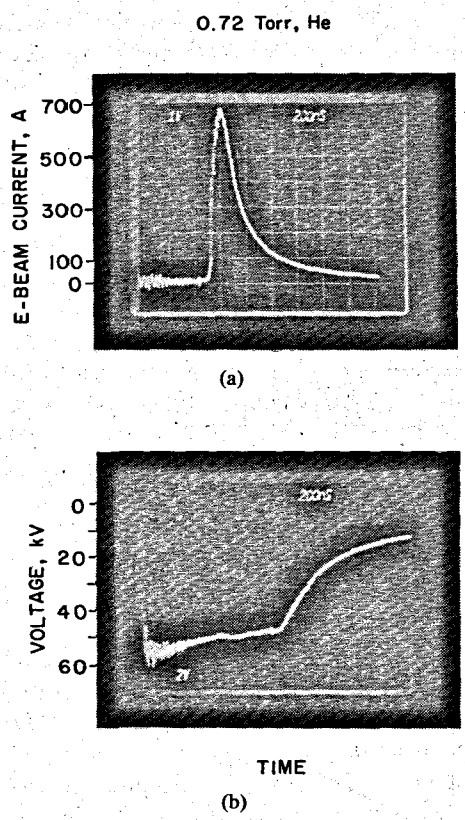

Fig. 4. (a) Electron beam current pulse. (b) Corresponding evolution of the discharge voltage. An aluminum cathode was used at 710 mtorr of He + 10 mtorr of O_2. The photographs were obtained in different pulses at the same discharge conditions. Pulse-to-pulse variation was negligible. The change in the slope of the voltage pulse corresponds to the instant of discharge breakdown; the initial linear drop is due to charge losses from the Marx generator capacitors before breakdown.

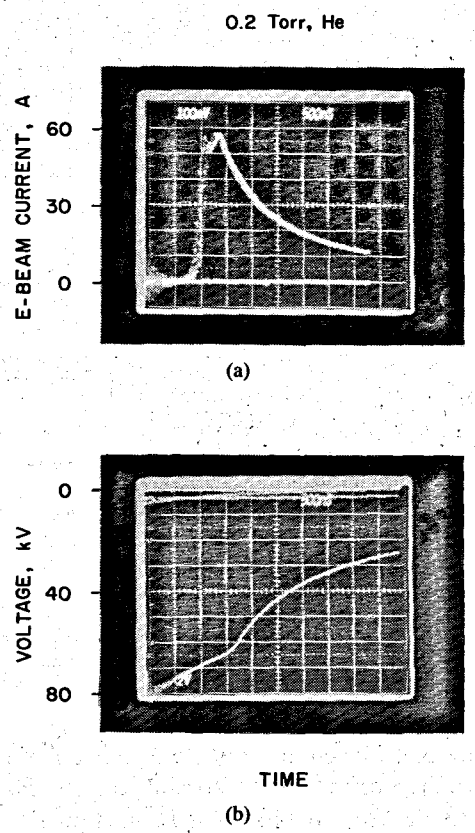

Fig. 5. (a) Electron beam current pulse. Three superimposed traces can be seen. (b) Corresponding evolution of the discharge voltage. An aluminum cathode was used at 190 mtorr of He + 10 mtorr of O_2. The photographs were obtained in different pulses at the same discharge conditions. Pulse-to-pulse variation was negligible. The change in the slope of the voltage pulse corresponds to the instant of discharge breakdown; the initial linear drop is due to charge losses from the Marx generator capacitors before breakdown.

trates a lower current electron beam pulse of 1.6 μs FWHM and the discharge voltage variation. At lower discharge currents electron beam pulses of longer duration, lasting a few tens of microseconds, were recorded.

The electron beam current passing through a 7.7-μm-thick aluminum foil was measured using the 5-cm-ID current monitor. The foil was mounted on a stainless steel plate having an orifice of 2.8 cm in diameter placed in the axis of the discharge between the cathode and the coil. Results obtained operating the discharge at 100 kV at pressures between 100 mtorr and 300 mtorr are shown in Fig. 6. A transmitted beam current density of 9 A/cm^2 was measured at 300 mtorr. The energy cutoff of the filtering foil is 28 keV [9]. The results of the sheath model presented in Section IV show that the major part of the electron beam energy is carried by high-energy electrons with energy within 10 percent of that corresponding to the discharge voltage.

The aluminum cathode was also operated in pure oxygen and pure nitrogen atmospheres. Fig. 7(a), (b) shows the variation of the electron beam current passing through the 5-cm-diameter current monitoring coil as a function of discharge pressure and voltage. For both molecular gases, the maximum pressures at which an electron beam was generated were below 60 mtorr, and the maximum

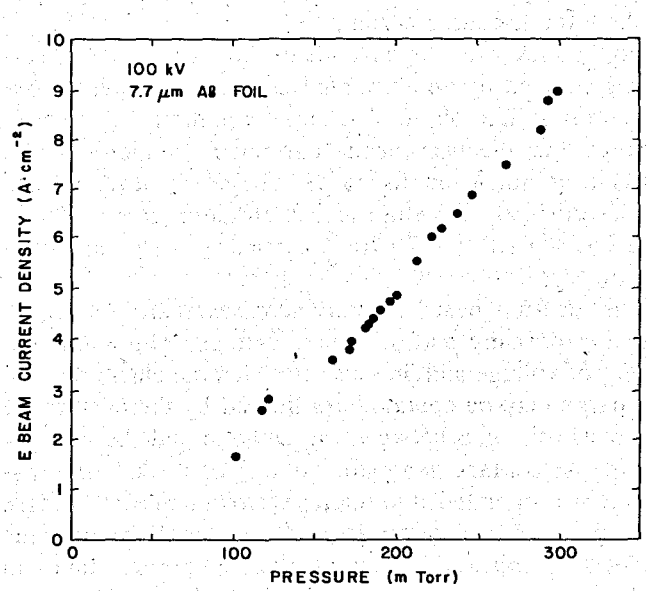

Fig. 6. Electron beam peak current density passing through a 7.7-μm-thick aluminum foil placed at 7 cm from the cathode as function of discharge pressure. The filtering foil has an energy cutoff of 28 keV. Measurements were made through an on-axis aperture 2.8 cm in diameter. Increasing pressure corresponds to increasing discharge current. An aluminum cathode was used in a He + 10 mtorr O_2 atmosphere. The Marx output voltage was 100 kV.

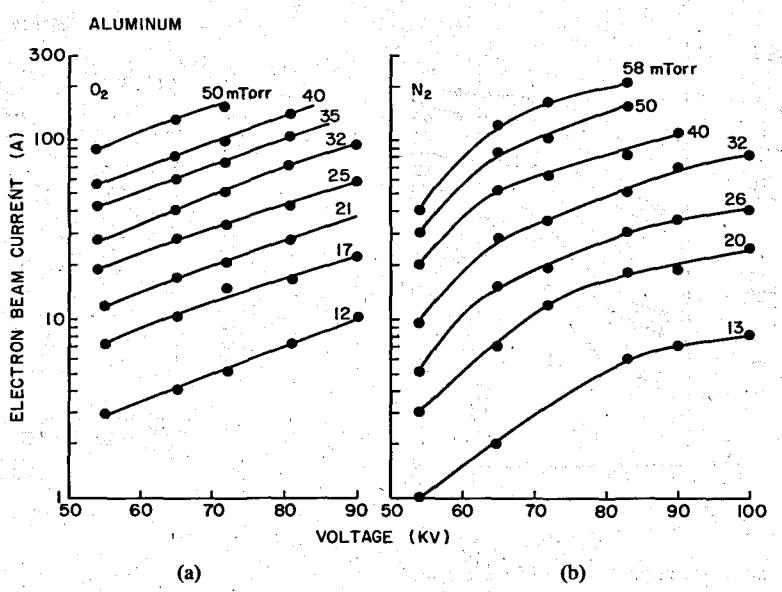

Fig. 7. Electron beam peak current versus initial voltage of the erected Marx generator, with pressure as a parameter. An aluminum cathode was used in (a) pure O_2, (b) pure N_2. In both cases a 5-cm-ID pulse transformer was used to measure the current at 7 cm from the cathode.

electron beam current obtained in both cases was below 200 A.

The use of magnesium as a cathode material was also investigated. As in the case of aluminum, magnesium forms oxide or nitride layers that constitute efficient emitters of electrons following ion bombardment. Fig. 8 shows the variation of the electron beam current as a function of discharge voltage and pressure. As in Fig. 3, the gas mixture contained 10 mtorr of oxygen, the balance being helium. The electron beam currents passing through the 5-cm monitoring coil are comparable to the values obtained with the aluminum cathode. A maximum current of 700 A was obtained at 65 kV and a pressure of 520 mtorr.

Fig. 9(a), (b) shows the electron beam currents obtained operating the magnesium cathode in pure oxygen and nitrogen atmospheres, respectively. In these experiments the maximum electron beam current measured through the 5-cm coil was below 200 A. As in the case of aluminum, the electron beam currents obtained in the oxygen and nitrogen atmospheres are considerably lower than those obtained in the helium–oxygen mixture.

We also studied glow discharges generated using a molybdenum cathode. In contrast with aluminum and magnesium, molybdenum does not form oxide or nitride layers that significantly increase electron emission. Fig. 10 summarizes the electron beam currents obtained in a helium atmosphere. Fig. 11(a), (b) shows the results obtained in experiments in pure oxygen and nitrogen atmospheres, respectively. In all cases, the currents emitted by the molydenum cathode are significantly lower than those obtained with the oxidized cathodes. All the results discussed in the following sections were obtained using aluminum cathodes.

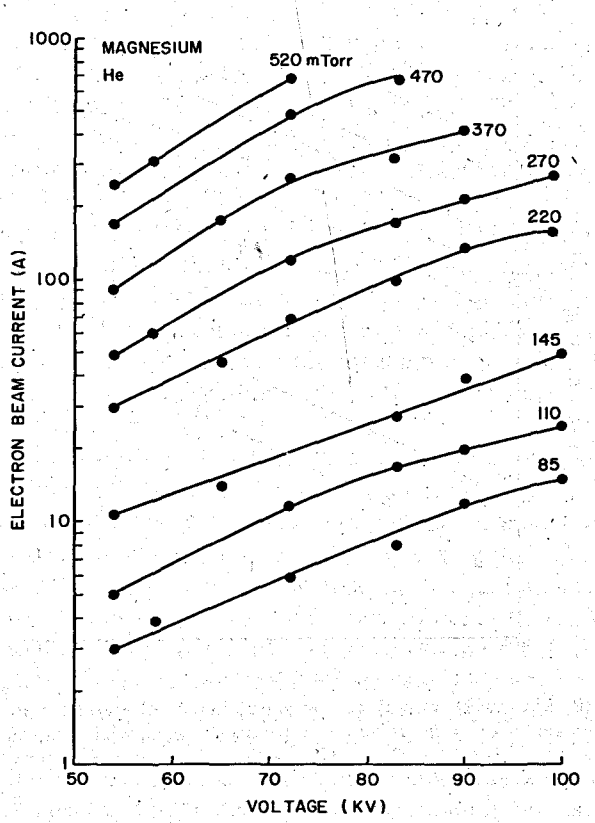

Fig. 8. Electron beam peak current versus initial voltage of the erected Marx generator, with pressure as a parameter. The magnesium cathode was used in He + 10 mtorr of O_2. A 5-cm-ID pulse transformer was used to measure the current at 7 cm from the cathode.

B. Spatial Distribution of the Electron Beam Current

We have studied the radial and axial variation of the electron beam current. All the experiments discussed in this section were performed in a helium–oxygen atmo-

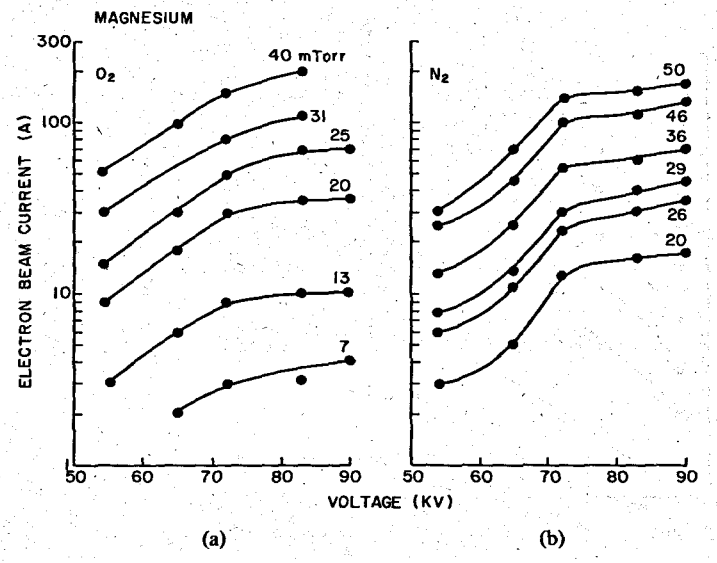

Fig. 9. Electron beam peak current versus initial voltage of the erected Marx generator, with pressure as a parameter. A magnesium cathode was used in (a) pure O_2, (b) pure N_2. In both cases a 5-cm-ID pulse transformer was used to measure the current at 7 cm from the cathode.

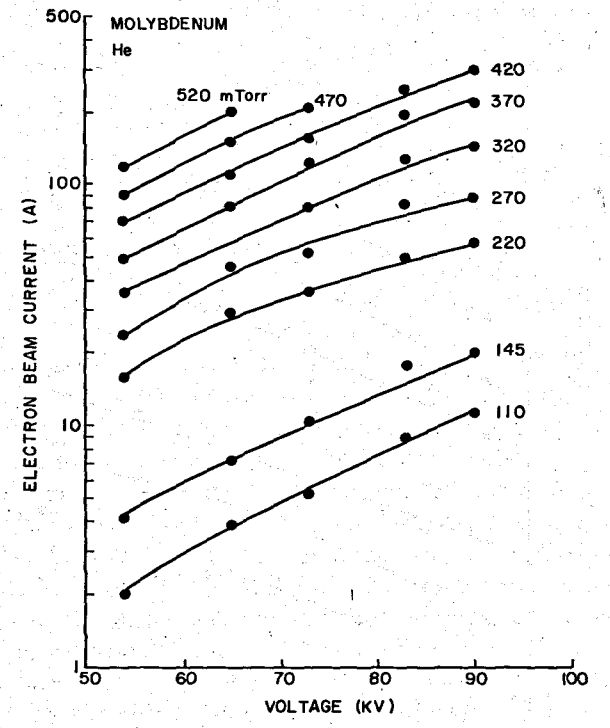

Fig. 10. Electron beam peak current versus initial voltage of the erected Marx generator, with pressure as a parameter. A molybdenum cathode was used in He + 10 mtorr of O_2. A 5-cm-ID pulse transformer was used to measure the current at 7 cm from the cathode.

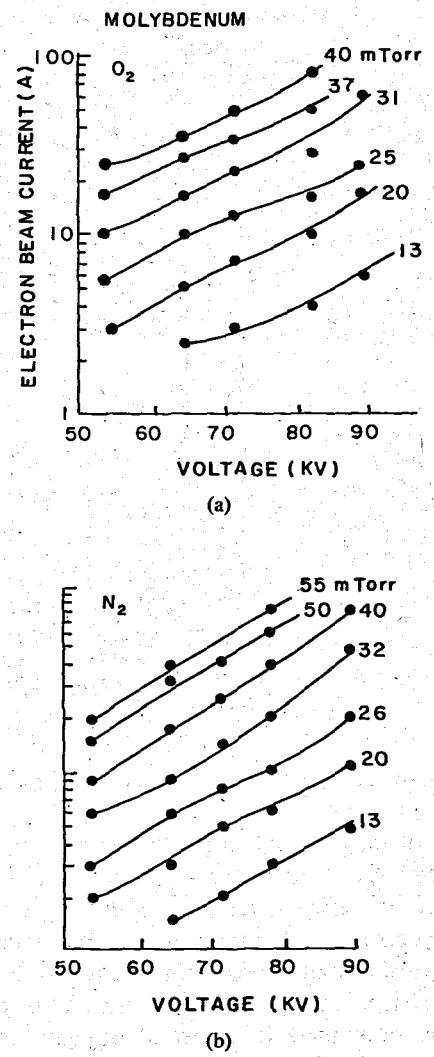

Fig. 11. Electron beam peak current versus initial voltage of the erected Marx generator, with pressure as a parameter. A molybdenum cathode was used in (a) pure O_2, (b) pure N_2. In both cases a 5-cm-ID pulse transformer was used to measure the current at 7 cm from the cathode.

sphere. The radial distribution was measured displacing the 1.25-cm-diameter coil masked by a stainless steel plate across a cathode diameter by means of a vacuum feedthrough. The plate supported two blades defining a 1.25 $\times$ 0.2 cm^2 slot that provided good spatial resolution. The electron beam current profile was measured monitoring the current passing through the slot at different positions. When using this configuration to measure the electron beam current in the region close to the axis of the discharge two very distinct groups of current pulses were observed for a given discharge condition. One group of pulses is distinguished by an anomalously high current. These pulses were determined to be due to the presence of a small-diameter (0.5 mm) high-current-density (1000 A/cm^2) beam of electrons. The position of this minibeam was observed to change slightly from shot to shot, but was always observed to appear near the center of the discharge. Even if the current contribution of this small beam is only several amps, it can distort the electron beam current radial profiles and should be taken into account in analyzing the current distribution profiles. Anomalously high currents pulses were measured in the shots in which the position of this minibeam was coincident with the slot. The characteristics of this small diameter beam of electrons is further discussed in Section III-D.

The solid lines in Fig. 12 show the radial distributions of the electron beam current measured at 7 cm from the cathode corresponding to discharge currents of 100 and

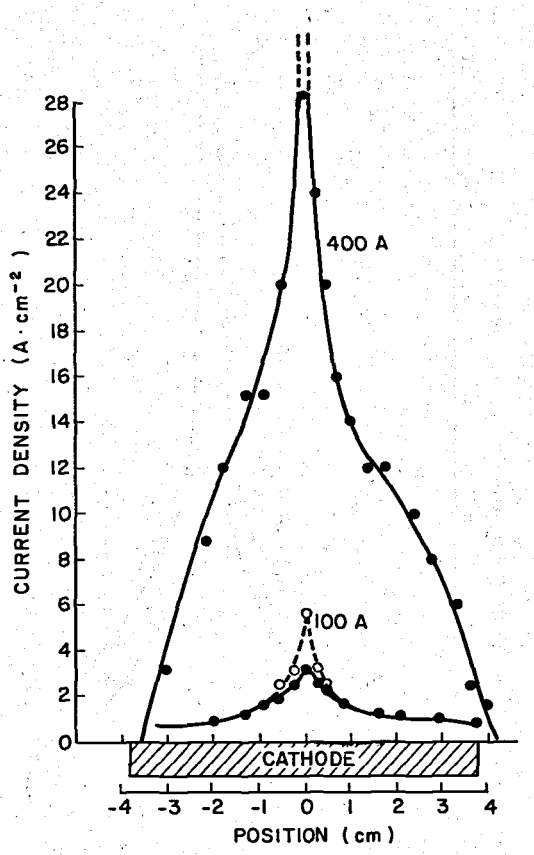

Fig. 12. Radial distribution of electron beam peak current density measured at 7 cm from the aluminum cathode for two values of the discharge current. A slotted mask of 1.25 × 0.2 cm^2 was used in front of the current monitor. The full lines correspond to data obtained in the absence of the minibeam. The dashed lines relate data points obtained in the presence of the minibeam. In the 400-A profile, the near axis values in the presence of the minibeam reach 80 A/cm^2 and fall out of scale. The shadowed region in the abscissa identifies the relative position of the cathode.

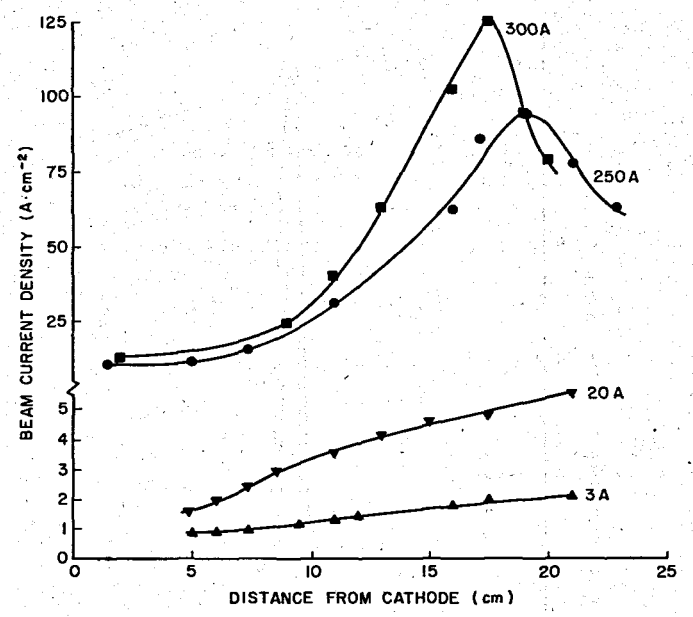

Fig. 13. Electron beam current density profile along the axis of the beam, measured using a 1.25-cm-diameter coil. The discharge voltage was 72 kV. A change of scale was used in the current density axis, to allow the comparison of the four curves. Peak discharge currents are indicated.

400 A in the absence of the minibeam. The shape of the profile measured by O'Brien [7] for a 180-cm^2 aluminum cathode operated at a current of 34 A was very uniform. Our measurements at a larger current of 100 A show an electron beam profile that is slightly more intense at the axis. When the current was further increased to 400 A a distribution sharply peaked at the axis was obtained. The current calculated by integrating the 5-cm central region under the respective profiles agrees within 10 percent with the current measured with the 5-cm-diameter pulse transformer, at the same discharge conditions.

The dashed lines in Fig. 12 relate to measurements in which the position of the minibeam was coincident with the slot and were obtained in several pulses by displacing the current probe as described above. The data points, symbolized with open circles, include the current contribution of the minibeam and appear to increase the current density of the electron beam in the axis of the discharge. However, a better description of the current distribution for a given pulse is the one described by the solid lines with the addition of a very narrow (0.5 mm) peak at some specific location near the axis of the discharge within the region corresponding to the dashed lines in Fig. 12.

Fig. 13 shows the current density variation along the electron beam axis for four values of the discharge current measured with the 1.25-cm-diameter coil. The electron beam current density at the axis is seen to increase as a function of the distance from the cathode. At 300 A the entire beam focuses into a spot of a few square centimeters at 17.5 cm from the cathode surface. The location of the region of maximum current density at the axis approaches the cathode as the electron beam current increases. The variation of this location with discharge conditions agrees well with results of simple calculations of the beam constriction due to the self-generated magnetic field.

At high currents (>150 A) a bright, pink plasma is observed in the region where the highest current densities are attained. The electrostatic probe measurements discussed in Section III-C confirm that a higher density plasma (>5 10^{12} cm^{-3}) develops in this region. Strong beam–plasma interactions are likely to occur there. This phenomenon was previously observed in the focal region of glow-discharge-generated dc electron beams [10]. By this mechanism a significant fraction of the electron beam energy is transferred to the plasma, which increases both its density and temperature. Simultaneously, the electron beam spectrum degrades [10] and the beam diverges.

We have also studied the radial profiles of the beam after passing through a 7.7-μm-thick aluminum foil at 7 cm from the cathode. Figs. 14 and 15 compare the beam profiles with and without the foil at the same set of discharge voltage and $He–O_2$ operating pressure: at 100 kV and 100 mtorr, and at 100 kV and 200 mtorr, respectively. In both cases the integrated current passing through the foil is approximately 80 percent of the current evaluated from the profile without the foil. The acceptance an-

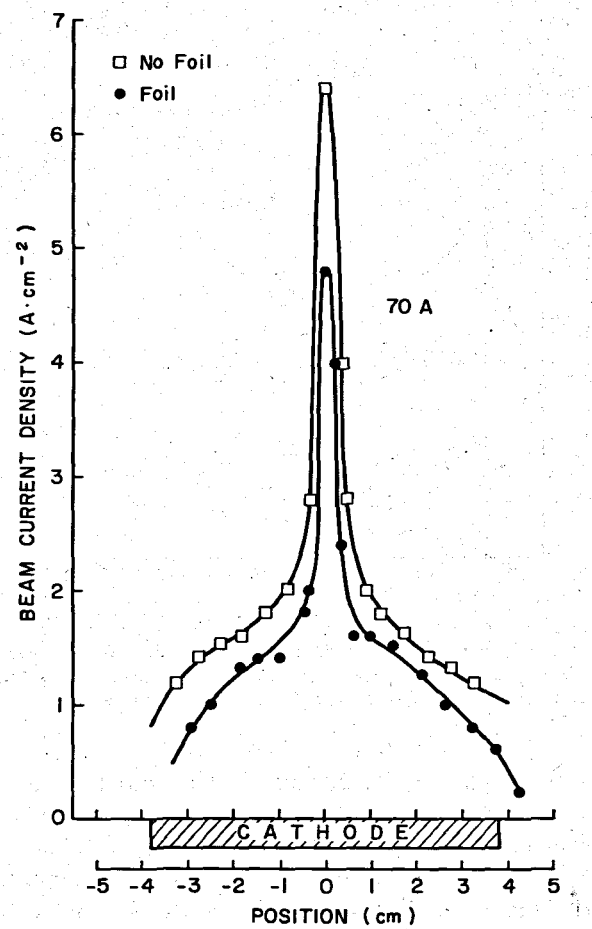

Fig. 14. Electron beam current radial profile measured with (lower trace) and without (upper trace) a 7.7-μm-thick Al foil placed between the cathode and the coil. The profile was measured with a slotted aperture of 0.2 × 1.25 cm^2 placed in front of a current monitoring coil at 7 cm from the cathode. The peak discharge current was 70 A.

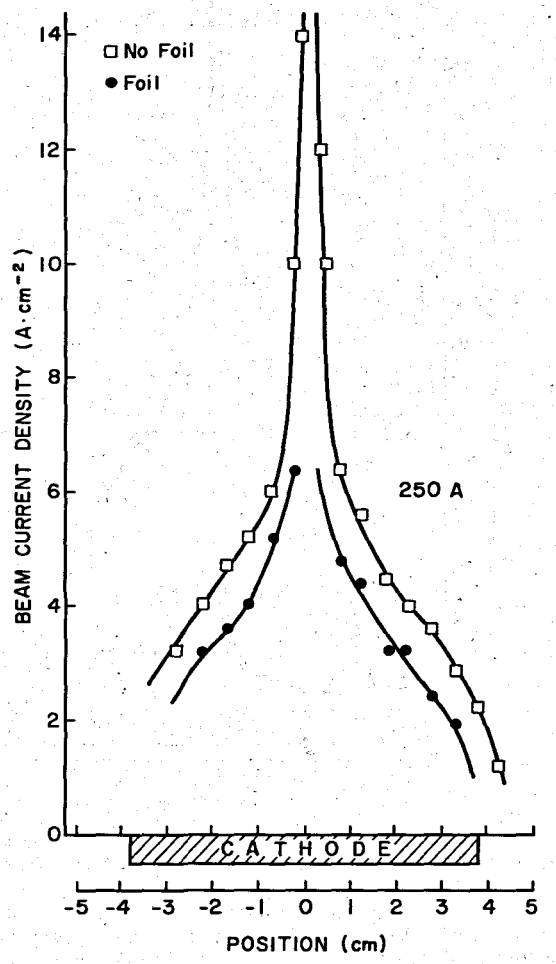

Fig. 15. Electron beam current radial profile measured with (lower trace) and without (upper trace) the 7.7-μm-thick Al foil placed between the cathode and the coil. The profile was measured with a slotted aperture of 0.2 × 1.25 cm^2 placed in front of a current monitoring coil at 7 cm from the cathode. The peak discharge current was 250 A.

gle of our detection system composed by the slot and the pulse transformer is rather small (12°). At 100 kV the fraction of fast electrons that are scattered by the foil at larger angles, thereby not reaching the detector, is calculated to be approximately 15 percent. Consequently, 95 percent of the total current is estimated to be composed of fast electrons that pass through the foil.

Sharp peaks in the electron beam current density distributions are observed at the axis of the electron beam in Figs. 14 and 15. As previously discussed, the origin of this phenomenon is the presence of a very small diameter (<1 mm) beam of energetic electrons approximately coincident with the axis of the high-current-density discharge. Thus, during the high-current-density measurements with the foil we avoided the axial region because the minibeam could perforate the foil. For this reason, the lower trace in Fig. 15 is open. This phenomenon is further discussed in Section III-D.

C. Electron Density and Temperature

The electron energy distribution in the negative glow of the discharge is non-Maxwellian, containing high-speed electrons that have been accelerated in the cathode fall [11]. A large fraction of these electrons have an energy corresponding to approximately the entire discharge voltage. The calculated energy distribution of these high-speed electrons is discussed in Section IV. Nevertheless, the majority of the electrons in the negative glow region have low energy. This low-energy group, which practically determines the plasma density, is made of secondary electrons produced by the beam electrons in ionizing collisions [11]. The energy distribution of these slow electrons is approximately Maxwellian [6], [7], [10].

The knowledge of the plasma density and electron temperature in the negative glow region of the discharge is relevant to the process of electron beam generation. These parameters determine the ion flux from the negative glow to the cathode fall region. These ions, which are subsequently accelerated in the cathode fall region, and the fast neutral atoms created by charge transfer collisions, are responsible for the emission of secondary electrons at the cathode surface. In the rest of this section we discuss the measurement of the temperature and density of the thermalized electrons. In Section IV we use these experimental values in a model of the discharge to predict the energy

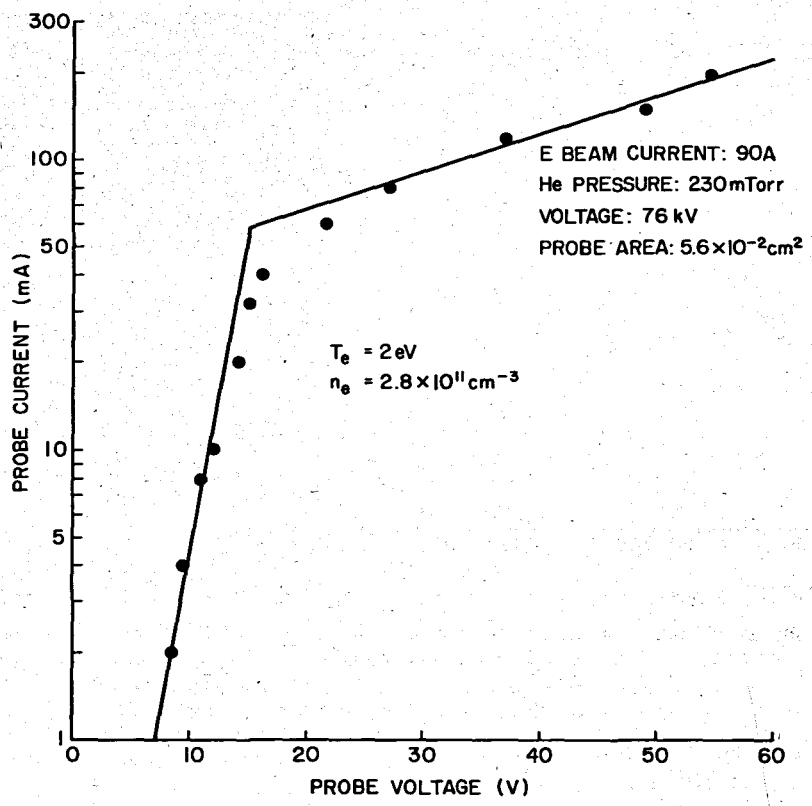

Fig. 16. Langmuir single-probe characteristic yielding plasma density and electron temperature. The measurements were performed at 20 cm from the cathode, at a discharge voltage of 76 kV, using an aluminum cathode in a helium–oxygen atmosphere at 230 mtorr.

distribution and density of beam electrons produced in the glow discharge.

McClure [6] and O'Brien [7] have previously measured the plasma density and electron temperature in the negative glow region of pulsed discharges. Their measurements correspond to low-discharge current densities (<0.3 A/cm^2). We have measured these parameters at glow discharge current densities up to 10 A/cm^2.

Our measurements were made using single and double electrostatic probes. The probe traces were obtained by sequentially changing the probe bias on a shot-by-shot basis. The double probe was used to measure in the high-density plasma region, where the electron beam focuses. The single probe, giving a larger signal, was used to measure the plasma parameter in the lower density regions. Our double probe has a better frequency response than our single probe. However, in measurements made in the plasma regions where it was possible to compare both probes, the values of the plasma parameters agree within a factor of two. Fig. 16 is a typical single probe trace, and corresponds to a measurement taken at 20 cm from the cathode.

Radial profiles of the plasma densities measured at 7 cm from the cathode using a single probe are shown in Fig. 17. The measurements were made at a discharge voltage of 72 kV and at currents of 180 and 450 A. The general shape of the plasma density profiles resembles the radial distribution of the electron beam current density

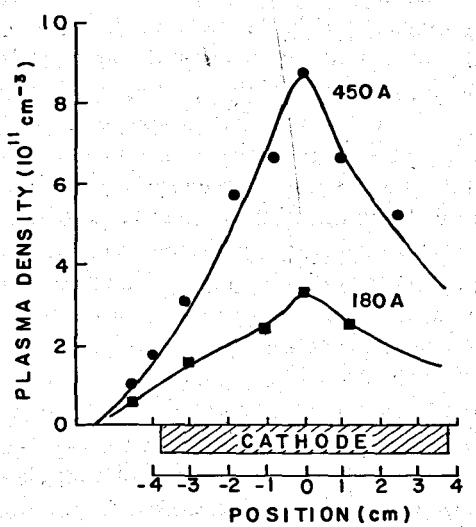

Fig. 17. Radial profiles of the plasma density measured at 7 cm from the cathode. Peak values of the discharge current are indicated.

shown in Fig. 12. The maximum plasma density is at the axis of the beam, where the electron beam current density peaks. Values of the electron temperature obtained from the same measurements were all between 1 and 1.5 eV.

The variation of the plasma density on the axis of the beam, at 7 cm from the cathode, as a function of discharge current is illustrated in Fig. 18. The measurements were obtained at a discharge voltage of 56 kV. In the range of currents investigated, the plasma density was observed

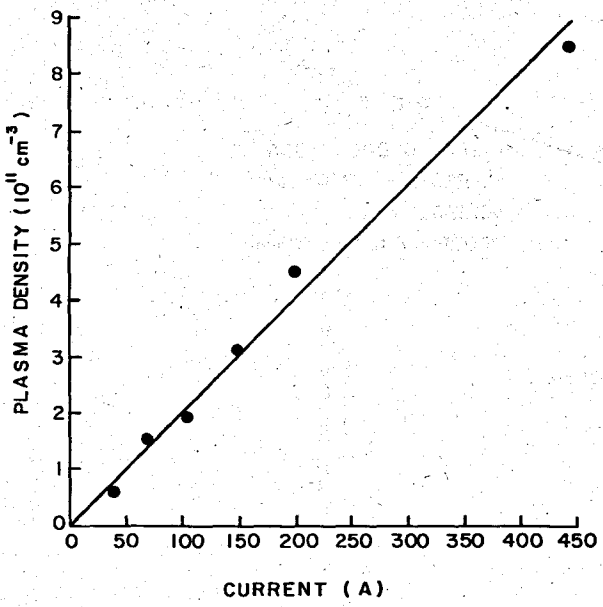

Fig. 18. On-axis plasma density as a function of the peak discharge current.

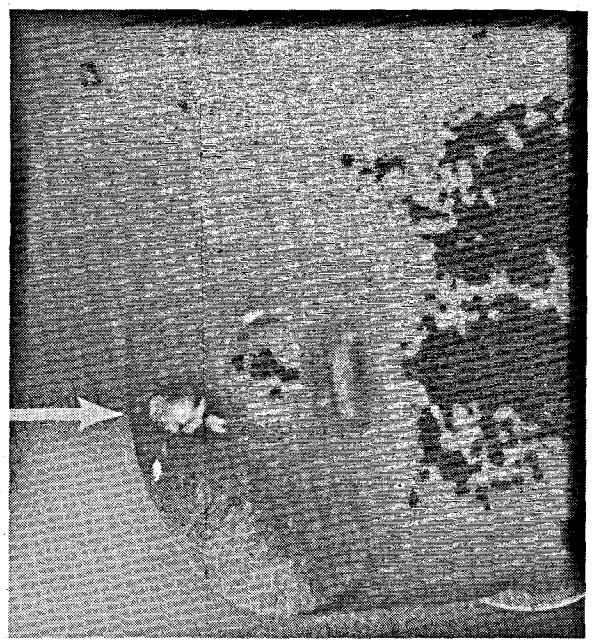

Fig. 19. Photograph of the plasma spot (arrow) generated when the minibeam impinges the brass wall of the 1.25-cm-ID pulse transformer. The coil was rotated 45° with respect to the beam axis to make it more visible. Discharge voltage was 82 kV, and the He + 10 mtorr O_2 pressure was 375 mtorr. The peak beam current was 300 A.

to increase linearly with the current, from a value of 6×10^{10} cm^{-3} at 40 A to 8.5×10^{11} cm^{-3} at 450 A. The electron energy values obtained from the same probe traces were also between 1 and 1.5 eV. In all the measurements made in the negative glow region of the discharge the plasma potential was between 5 and 10 V above anode potential, confirming that practically all the discharge voltage drops in the cathode sheath.

We also measured the plasma parameters at 20 cm from the cathode where at high currents a high luminosity plasma is observed. This is the region where, as shown in Fig. 13, the electron beam current density increases due to self-constriction. The energy of the thermal electrons in this region was observed to be consistently higher than closer to the cathode, where the electron beam current density is considerably lower. The measured electron energies in the high luminosity region are between 2 and 6 eV. Secondary electrons produced by ionization in the high luminosity region are likely to be heated as a result of beam–plasma interactions [10]. The plasma density in this region is also significantly higher. Values between 5×10^{12} and 7×10^{13} cm^{-3} were measured at electron beam currents between 160 and 400 A.

Measurements were also made in a pure nitrogen atmosphere at 7 cm from the cathode and 72 kV of discharge voltage. At a pressure of 30 mtorr and discharge current of 60 A (1.3 A/cm^2), we obtained an electron temperature $kTe = 1.2$ eV and a plasma density of 1.1×10^{11} cm^{-3}. At a pressure of 40 mtorr and discharge current of 100 A (2.2 A/cm^2), these values were 1.4 eV and 2×10^{11} cm^{-3}. These electron temperatures compare well with the value of $kTe = 1$ eV measured by O'Brien [7] at lower current densities (0.3 A/cm^2). The plasma densities measured in both experiments indicate the same linear increase with the current density.

D. High Current Density Mini-Electron Beam

As mentioned in Section III-B, a high-current-density electron beam of small diameter develops approximately in the axis of the discharge. This small beam made marks of less than 1 mm in diameter in the stainless steel blades used as collimators in the current profile measurements. As the coil was moved vertically across the cathode diameter, a line of similar dots was etched on the stainless steel plate used to protect the pulse transformer from electron bombardment.

Where this well-collimated minibeam impinges on a metallic surface, a bright plasma spot is observed. This effect is shown in Fig. 19. To obtain this photograph the coil was rotated 45° with respect to the axis of the discharge to permit viewing of the minibeam-created plasma. The photograph was obtained at a discharge voltage of 82 kV, in an He–O_2 mixture at 375 mtorr.

When the time evolution of the electron beam in the axial region of the beam was measured, the pulse shape shown in Fig. 20 was observed. This signal was obtained with a 1.25-cm-diameter current monitoring coil aligned with the axis of the discharge. A short pulse, having a width of approximately 20 ns, is apparent in the leading edge of the electron beam pulse. This feature is only observed in the axial region of the discharge where the minibeam is present, and consequently it is attributed to it.

Using data from Figs. 15 and 20 it is possible to obtain a rough estimate of the current and energy density of the minibeam. In Fig. 15 the current density at the center of the profile made without the aluminum foil is out of scale. The value there is 32 A/cm^2, and the major fraction is attributed to the minibeam. The corresponding measured

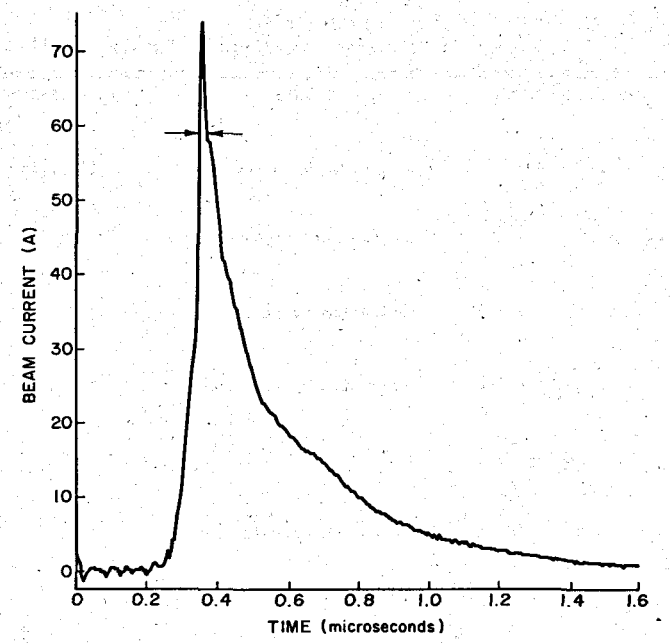

Fig. 20. Time evolution of the current in the central region of the electron beam. The signal was digitalized in 512 channels with 5-ns resolution. The minibeam is apparent between the arrows, and lasts about 20 ns. The He + 10 mtorr O_2 pressure was 430 mtorr and the discharge voltage was 72 kV.

current through the 0.2 × 1.25 cm^2 slot was 8 A. The base of the narrow peak in Fig. 15 can be estimated to be 7.5 A/cm^2, corresponding to a current of approximately 2 A. Consequently, the current of the minibeam at these discharge conditions is estimated to be 6 A. From the marks left in the stainless steel plate the diameter of the minibeam is estimated to be 0.5 mm. The corresponding current density is of the order of 1 kA/cm^2. Considering a pulsewidth of 20 ns and a discharge voltage of 100 kV, the energy density of this small beam can be estimated to be of the order of several joules per square centimeter.

Similar effects were also observed in magnesium cathodes when the discharge currents were above a few hundred amperes. Moreover, the plasma spot shown in Fig. 19 was found independent of the axial position of the target: A more detailed study is needed to determine the mechanism of formation of this high-current-density very-small-area electron beam.

IV. Model of the Electron Beam Generation

The pulsed glow discharges discussed in the previous section were operated at high current densities (1–20 A/cm^2) and at relatively high helium pressures. The mechanisms of electron beam generation at these conditions have not been previously studied.

We have modeled the process of electron beam generation in these high-current-density helium glow discharges. The model was used to predict the density and energy distribution of the electron beam. The results also show that fast neutral atoms bombarding the cathode make a major contribution to the total electron emission. We constructed a model of the cathode fall region similar to that previously developed by McClure [12] for a deuterium discharge. Our experimental values of the parameters of the negative glow region of the discharge were used to calculate the flux of ions entering the cathode sheath. The electric field and the fluxes of charged particles in the cathode fall region were calculated in a self-consistent manner. Charged particle pair creation in the sheath resulting from ionization by fast ions and beam electrons was included. The collisional processes considered in the cathode fall region include the creation of fast neutral atoms by charge transfer and are summarized in Table I. The sources of the cross-section data used are also indicated.

The secondary electron emission coefficients for aluminum under He^+ bombardment measured by Bourne *et al.* [13] were used. The secondary emission yields due to fast helium atoms and ions of the same energy were assumed to be equal for energies above 20 keV [14], but electron emission due to atoms was assumed to be negligible for energies below 500 eV.

The electron beam energy distribution resulting from running the model at 52 kV and 370 mtorr of helium is shown in Fig. 21. The conditions correspond to a measured negative glow plasma density at 4.5 × 10^{11} cm^{-3}, and electron energy of 1.5 eV. By integrating the data shown in Fig. 21, we calculated that 97 percent of the electron beam energy is carried by electrons having an energy that is within 10 percent of that corresponding to the discharge voltage. The low-energy peak is due to electrons created by ionization in the sheath. The integration of the total electron flux density amounts to a current den-

TABLE I
COLLISIONAL PROCESSES IN THE CATHODE SHEATH

REACTION	PROCESS	REFERENCE
$e + He \rightarrow He_s^+ + 2e$	Ionization by electrons	[15],[16]
$e + He \rightarrow He_s^{++} + 3e$	Double ionization by electrons	[17]
$He_f + He \rightarrow He_f^+ + He + e$	Ionization by fast neutrals	[18],[19]
$He_f^+ + He \rightarrow He_f^+ + He^+ + e$	Ionization by fast ions	[18],[19],[20]
$He_f^{++} + He \rightarrow He_s^+ + He_f^{++} + e$	Ionization by double ions	[17]
$He_f^+ + He \rightarrow He_f^{++} + He + e$	Ionization of fast ions	[18]
$He_f^+ + He \rightarrow He_f + He^+$	Ion-neutral charge-transfer	[18],[21],[22]
$He_f^{++} + He \rightarrow He_f + He^{++}$	Double ion-neutral double charge transfer	[23],[24],[25]
$He_f^{++} + He \rightarrow He_f^+ + He^+$	Double ion charge-transfer	[23],[24],[25]

s : slow particle

f : fast particle

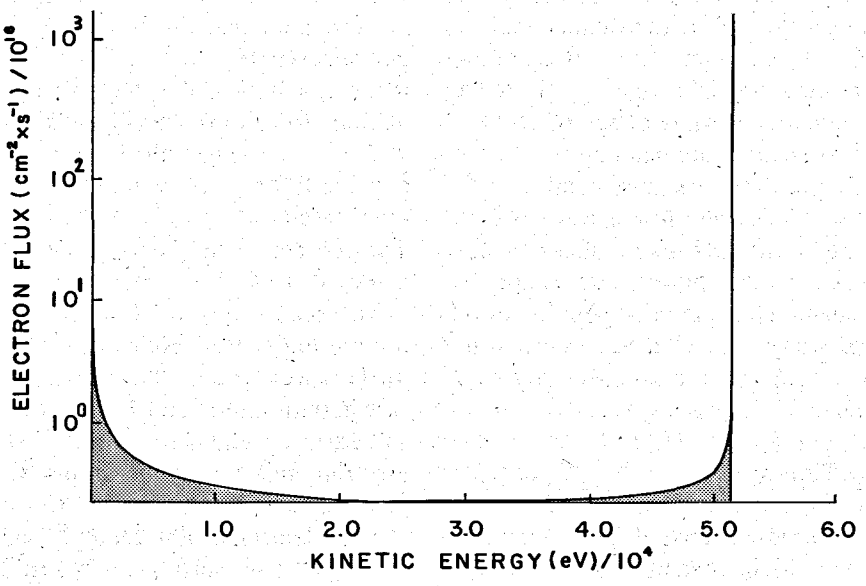

Fig. 21. Calculated electron flux energy distribution corresponding to a discharge voltage of 52 kV and a helium pressure of 350 mtorr.

sity of 4.1 A/cm^2. This value is in good agreement with the experimentally measured value of 4.5 A/cm^2.

Fig. 22(a), (b) shows the predicted energy spectra of the fluxes of He^+ and fast He atoms at the cathode. The emission rate of electrons is calculated by the convolution of these curves with the corresponding secondary electron emission data. For the above conditions the emission of electrons at the cathode due to fast neutrals is calculated to be 65 percent of the total electron emission at the cathode.

The model results can be summarized as follows. The electron beam current densities predicted using measured

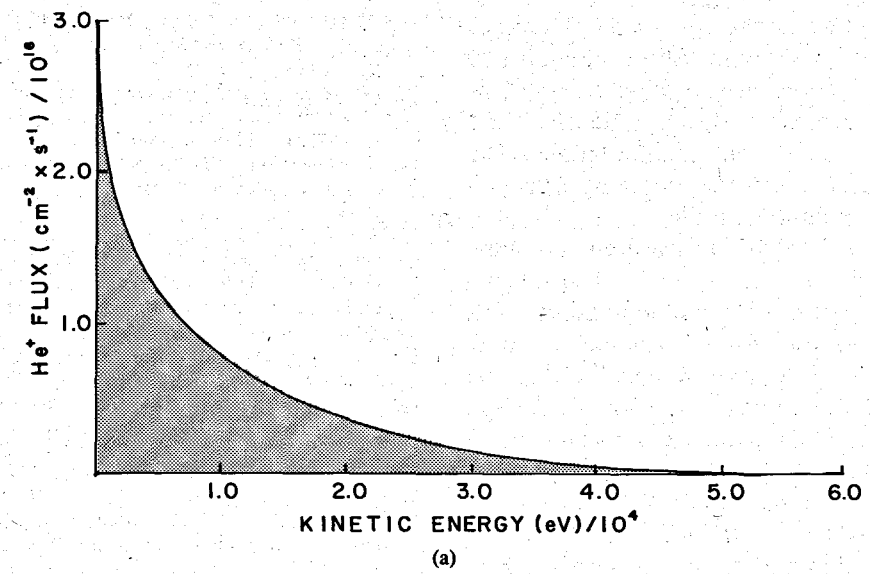

(a)

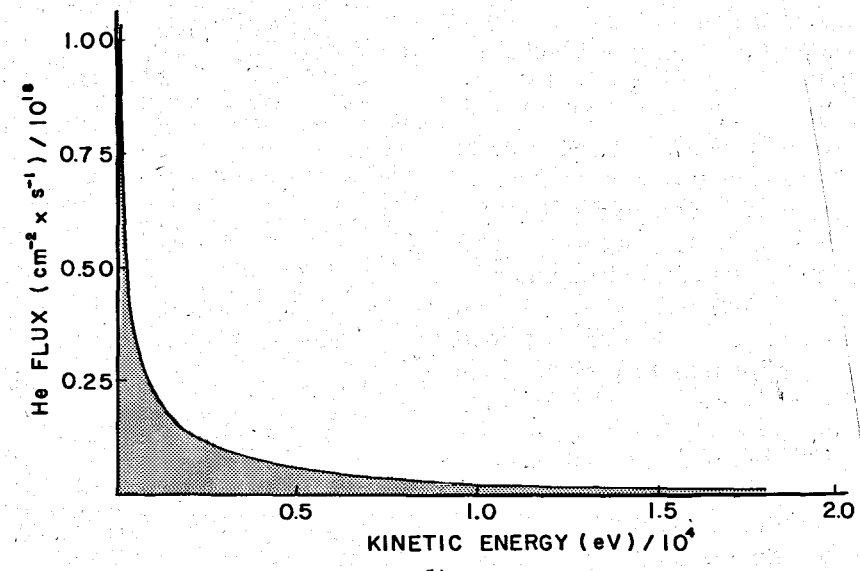

(b)

Fig. 22. (a) Calculated He^+ flux energy distribution at the cathode surface. (b) Calculated neutral helium flux energy distribution at the cathode surface. The distributions correspond to a discharge voltage of 52 kV and a helium pressure of 350 mtorr.

negative glow plasma parameters are of the same order as the experimental values. Fast neutral atoms, created by charge transfer in the cathode sheath, are at least as important as ions in causing the emission of electrons from the cathode surface. The emission due to neutrals results in electron beam current densities above those corresponding to the Child–Langmuir space-charge-limited ion flux for a given voltage and sheath thickness. More than 95 percent of the electron beam energy is carried by electrons having an energy that is within 10 percent of that corresponding to the discharge voltage.

V. Summary

We studied the generation of intense pulsed electron beams in glow discharges at voltages between 48 and 100 kV using cathodes 7.5 cm in diameter. An aluminum cathode in a helium–oxygen atmosphere produced electron currents up to 900 A (20 A/cm^2). Pulse duration was limited by the stored energy in the Marx generator. A current density of 9 A/cm^2 was measured through a 7.7-μm-thick aluminum foil in the axis of a 100-kV discharge. Similar current densities were obtained using an oxidized magnesium cathode. Arcs developing between the cathode and the ceramic shield set a limit for the maximum electron beam current and voltage. The electron beam currents obtained operating the discharge in pure oxygen and nitrogen atmospheres were lower than those obtained in the helium–oxygen mixture. A molybdenum cathode, which does not have a high electron yield oxide layer, delivered considerably lower current densities.

Simultaneously, the glow discharges were observed to generate a small-diameter (<1 mm) short-duration (20 ns) beam of energetic electrons of very high current density (>1 kA/cm^2) in the axis. Its energy density (>1 J/cm^2) is enough to etch marks on metallic targets. The understanding of the mechanism of formation of this intense small beam requires further studies.

Electron beam current distribution measurements show that the beam is relatively uniform at low (<100 A) currents. At large currents, self-constriction increases the axial beam density. Electrostatic probe measurements show that the negative glow plasma density and the electron beam current have a similar radial distribution. The plasma density measured at the axis of the discharge at 7 cm from the cathode increases linearly with discharge current. The electron temperature in the same region was measured to be between 1 and 1.5 eV. A bright high-density plasma was observed in the region where the highest electron beam current densities occur. Electrostatic probe measurements show that both the plasma density and the electron temperature are higher there than in the other regions of the discharge. This is possibly due to the onset of beam–plasma instabilities.

A model of the cathode sheath predicts electron beam current density values in agreement with the experiments. According to the model results, more than half of the electron current emitted at the cathode is due to the bombardment of fast neutral atoms created by charge transfer in the cathode sheath. The calculated energy distribution shows that >95 percent of the electron beam is carried by electrons having an energy within 10 percent of the discharge voltage.

Acknowledgment

The authors want to thank the experimental assistance of B. Wernsman and the skillful machining by J. Davis. The support and the helpful comments by A. Garscadden and P. Haland are gratefully acknowledged.

References

[1] A. S. Pokrovskaya-Soboleva and B. N. Kliarfel'd, "Ignition of the high voltage discharge in hydrogen at low pressures," *Sov. Phys.—JETP*, vol. 5, pp. 812–818, Dec. 1957.

[2] R. A. Dugdale, "Soft vacuum processing of materials with electron beams," *J. Mater. Sci.*, vol. 10, pp. 896–902, 1975.

[3] J. J. Rocca, J. D. Meyer, M. R. Farrell, and G. J. Collins, "Glow-discharge-created electron beams: Cathode materials, electron gun designs, and technological applications," *J. Appl. Phys.*, vol. 56, pp. 790–797, Aug. 1984.

[4] B. Wernsman, H. F. Ranea-Sandoval, J. J. Rocca, and H. Mancini, "Generation of pulsed electron beams by simple cold cathode plasma guns," *IEEE Trans. Plasma Sci.*, vol. PS-14, no. 4, pp. 518–522, Aug. 1986.

[5] J. J. Rocca, J. D. Meyer, Z. Yu, M. Farrell, and G. J. Collins, "Multikilowatt electron beams for pumping CW lasers," *Appl. Phys. Lett.*, vol. 41, pp. 811–813, Nov. 1982.

[6] G. W. McClure, "High-voltage glow discharges in D_2 gas. I. Diagnostic measurements," *Phys. Rev.*, vol. 124, pp. 969–982, Nov. 1961.

[7] B. B. O'Brien, Jr., "Characteristics of a cold cathode plasma electron gun," *Appl. Phys. Lett.*, vol. 22, pp. 503–505, May 1973.

[8] G. G. Isaacs, D. L. Jordan, and P. J. Dooley, "A cold-cathode glow discharge electron gun for high-pressure CO_2 laser ionisation," *J. Phys. E: Sci. Instrum.*, vol. 12, pp. 115–118, 1979.

[9] M. J. Berger and S. M. Seltzer, *Tables of Energy-Losses and Ranges of Electrons and Positrons*, NAS-NRC Pub. 1133, p. 205, 1964.

[10] Z. Yu, J. J. Rocca, and G. J. Collins, "Studies of a glow discharge electron beam," *J. Appl. Phys.*, vol. 54, pp. 131–136, Jan. 1983.

[11] Z. Yu, J. J. Rocca, G. J. Collins, and C. Y. She, "The energy of thermal electrons in electron beam created helium discharges," *Phys. Lett.*, vol. 96A, pp. 125–127, Jun. 1983.

[12] G. W. McClure and K. D. Granzow, "High-voltage glow discharges in D_2 gas. II. Cathode fall theory," *Phys. Rev.*, vol. 125, pp. 3–10, Jan. 1962.

[13] H. C. Bourne, Jr., R. W. Cloud, and J. G. Trump, "Role of positive ions in high-voltage breakdown in vacuum," *J. Appl. Phys.*, vol. 26, pp. 596–599, May 1955.

[14] F. Schwirtzke, "Ionisierungs-und Umladequerschnitte von Wasserstoff-Atomen und Ionen von 9 bis 60 keV in Wasserstoff," *Z. Physik*, vol. 157, pp. 510–522, 1960.

[15] W. Lotz, "Electron-impact ionization cross sections and ionization rate coefficient for atoms and ions," *Astrophys. J.* (Suppl. Ser. XIV), no. 128, pp. 207–237, May 1967.

[16] L. J. Kiefer and G. H. Dunn, "Electron impact ionization cross section data for atoms, atomic ions and diatomic molecules: I. Experimental data," *Rev. Mod. Phys.*, vol. 38, pp. 1–35, Jan. 1966.

[17] M. J. Van Der Wiel, F. J. DeHeer, and G. Wiebes, "Double ionization of helium," *Phys. Lett.*, vol. 24A, pp. 423–424, Apr. 1967.

[18] S. K. Allison, "Experimental results on charge-changing collisions of hydrogen and helium atoms and ions at kinetic energies above 0.2 keV," *Rev. Mod. Phys.*, vol. 30, pp. 1137–1138, Oct. 1958.

[19] L. J. Pucket, G. O. Taylor, and D. W. Martin, "Cross sections for ion and electron production in gases by 0.15–1.00 MeV hydrogen and helium ions and atoms," *Phys. Rev.*, vol. 136, pp. 379–385, Oct. 1964.

[20] R. A. Langley, D. W. Martin, D. S. Harmer, J. W. Hooper, and E. W. McDaniel, "Cross sections for ion and electron production in gases by fast helium (0.133–1.0 MeV): I. Experimental," *Phys. Rev.*, vol. 36, pp. 379–385, Oct. 1964.

[21] S. W. Nagy, W. J. Savloa, Jr., and E. Poylack, "Measurements of the total cross section for symmetric charge exchange in helium from 400–2000 eV," *Phys. Rev.*, vol. 177, pp. 71–76, Jan. 1969.

[22] J. B. Hasted, in *Atomic and Molecular Processes*, D. R. Bates, Ed. New York: Academic, 1962, pp. 496–720.

[23] K. H. Berkner, R. V. Pyle, J. W. Stearns, and J. C. Warren, "Single and double electron capture by 7.2 to 181 keV He^{++} ions in He," *Phys. Rev.*, vol. 166, pp. 44–46, Feb. 1968.

[24] G. R. Hertel and W. S. Koski, "Cross sections for the single charge transfer of doubly charged rare gas ions in their own gases," *J. Chem. Phys.*, vol. 40, pp. 3452–3453, 1964.

[25] L. I. Pivovar, M. T. Novikov, and V. M. Tubaev, "Electron capture of helium ions in various gases in the 300–1500 keV energy range," *Sov. Phys.—JETP*, vol. 15, pp. 1035–1037, Dec. 1962.